

# Anisotropic ferromagnetism and structure stability in $4f$ - $3d$ intermetallics: *ab initio* structure optimization and magnetic anisotropy for $\text{RCo}_5$ (R=Ce, La, and Y)

Munehisa Matsumoto

*Institute for Solid State Physics (ISSP), University of Tokyo, Kashiwa 277-8581, JAPAN*

(Dated: February 1, 2019)

Electronic mechanism in the interplay between ferromagnetism and structure stability of  $4f$ - $3d$  intermetallics in the main phase of rare-earth permanent magnets is investigated from first principles. We present a case study with an archetypical materials family  $\text{RCo}_5$  (R=Ce, La, Y), which was a part of the earliest rare-earth permanent magnets and from which other representative main-phase compounds can be regarded as a derived type. Comparison with the champion magnet materials family  $\text{R}_2\text{T}_{14}\text{B}$  and recently revisited materials family  $\text{RT}_{12}$  (T=Co and Fe) points to a direction leading to a mid-class magnet for the possible next generation materials.

PACS numbers: 75.30.Gw, 75.50.Ww, 75.10.Lp, 71.15.Rf

## I. INTRODUCTION

Rare-earth permanent magnet (REPM) obviously needs a good ferromagnet with sufficiently strong coercivity and robust structure. Unfortunately, cohesive energy and magnetic energy in magnetic materials do not quite behave in a synchronized way: too strong magnetization may stretch the lattice spacing too much via the magnetovolume effect for the chemical bonds to sustain the crystal structure. Thus a strong magnetization can ruin the structure stability. This makes one of the unavoidable trade-off situations in the materials design for permanent magnets. Careful inspection is needed to find out a best compromise with an optimal chemical composition and crystal structure to satisfy the prerequisites for permanent magnets. We do this on the basis of *ab initio* electronic structure theory, unearthing interplay in the middle of dual nature harboring both of delocalization and localization both in  $3d$ -electrons and in  $4f$ -electrons.

We focus on light rare-earth elements, R=Ce and La, motivated by their abundance and also in quest for a way to possibly exploit the subtlety in  $4f$ -electron physics to fabricate a new type of REPM's where half-delocalized  $4f$ -electrons contribute positively to the bulk magnetic properties. As a reference case without  $4f$ -electrons, R=Y is also addressed. The particular crystal structure of  $\text{RCo}_5$  makes a part of the building block for all of the other representative compounds,  $\text{R}_2\text{M}_{14}\text{B}^1$ ,  $\text{RM}_{12}$  and  $\text{R}_2\text{M}_{17}^2$  where M represents Fe-group elements.

In the next section, we describe our methods based on *ab initio* structure optimization utilizing the open-source package OpenMX<sup>3</sup>. In Sec. III, we present *ab initio* results on  $\text{RCo}_5$  (R=Ce, La, and Y) for their formation energy, magnetization, and magnetic anisotropy, being contrasted to the analogous data for the Fe-counterparts. Structure varieties and implications on the material-design principles for REPM's are discussed in Sec. IV. Conclusions and outlook are given in the final section.

## II. METHODS

Intrinsic magnetic properties of  $\text{RCo}_5$  and  $\text{RFe}_5$  (R=Ce, La, Y) are calculated from first principles via *ab initio* structure optimization utilizing the open-source software package OpenMX<sup>3-8</sup> on the basis of pseudopotentials<sup>9,10</sup> and the local orbital basis sets.

The lattice constants of Fe-group ferromagnets seems to be best described within Generalized Gradient Approximation (GGA) as proposed Perdew, Burke, and Ernzerhof (PBE)<sup>11</sup> and we present the results based on GGA-PBE. The basis set we take in OpenMX is Ce8.0-s2p2d2f1, La8.0-s2p2d2f1, Y8.0-s3p2d2f1, Fe6.0S-s2p2d1, and Co6.0S-s2p2d2f1 for  $\text{R}(\text{Co,Fe})_5$  within the given pseudopotential data set<sup>3</sup>. The energy cutoff is set to be 500 Ry of which choice has been inspected together with the basis sets to ensure a good convergence.

Similar basis sets with a few more or less inclusion of local basis wavefunctions can be good as well depending on the target materials and the issue being investigated as long as the choice of the basis set is coherently applied in a fixed scope of target materials and target observables. For the calculations of magnetic anisotropy energy presented below and elsewhere<sup>12</sup>, we have actually seen that slightly richer basis sets Ce8.0-s3p3d3f2 and La8.0-s3p3d3f2 work on a par with the basis sets written in the previous paragraph or sometimes in a better way especially when the target material is close to the verge of a delocalization-localization transition in  $4f$ -electrons. In the scope of the present work, presumably we stay on the side where the delocalized nature of  $4f$ -electrons dominates within the crystal structure of  $\text{CeCo}_5$ . For this purpose, either Ce8.0-s3p3d3f2 or Ce8.0-s2p2d2f1 will do basically.

The starting structure is taken from the experimentally measured lattice constants for  $\text{YCo}_5$ <sup>13</sup> and *ab initio* structure optimization is done for stoichiometric compounds  $\text{RCo}_5$  and  $\text{RFe}_5$  to get a minimized energy  $U_{\text{tot}}[\text{RT}_5]$  (T=Co, Fe) and the associated magnetization in the ground state. Thus extracted energy is used to

assess the structure stability by looking at the formation energy referring to the elemental materials which are analogously addressed with *ab initio* structure optimization by which the reference energies are extracted. The formation energy of  $\text{RCO}_5$ , which we denote by  $\Delta E[\text{RCO}_5]$ , is defined as follows:

$$\begin{aligned} \Delta E[\text{RCO}_5] \\ \equiv U_{\text{tot}}[\text{RCO}_5] - U_{\text{tot}}[\text{R per atom}] - 5U_{\text{tot}}[\text{Co per atom}] \end{aligned}$$

The structure optimization is done allowing for magnetic polarization without spin-orbit interaction. Then on top of the optimized lattice, magnetic anisotropy energy is investigated by fully relativistic calculations incorporating the spin-orbit interaction, putting a constraint on the direction of magnetization and numerically measuring the energy as a function of the angle between magnetization and crystallographic  $c$ -axis. Thus we look at the trends in the intrinsic properties focusing on the tradeoff between formation energy and magnetization, assisted by the data for magnetic anisotropy. As for the other prerequisite intrinsic property, Curie temperature, some of the issues and finite-temperature magnetism are addressed in separate works<sup>14–17</sup>.

### III. RESULTS

*Ab initio* structure optimization for  $\text{RCO}_5$ , elemental R (fcc-Ce, dhcp-La, hcp-Y) and elemental Co, that is, hcp-Co gives the energy and magnetization for each of the target systems within the given pseudopotential data sets. Calculated formation energy and magnetization from structure optimization runs are presented in Sec. III A and III B, respectively. Then in Sec. III C we show results from fully-relativistic calculations for magnetic anisotropy energy on top of the optimized lattice.

#### A. Formation energy

We start with inspecting the formation energy as a clue for the trend in the structure stability. Taking calculated energy within the particular choice of the basis set described in the previous section and given standard data sets of pseudopotentials<sup>3</sup>, calculated formation energy for  $\text{RT}_5$  (R=Y, La, Ce, and T=Co, Fe) is summarized in Fig. 1. The detailed procedures for the calculation of formation energy follow those described in Refs. 18 and 19. On the optimized lattice, the lattice constants and unit-cell volume have been read off as summarized in Table I. Comparing with the experimental data<sup>21</sup> which is available only for Co-based materials, it is seen that *ab initio* structure optimization predicts the realistic lattice constants and the unit cell volume within the precision of three significant digits.

We reproduce the known experimental fact that  $\text{RFe}_5$  is metastable<sup>20</sup> with the calculated formation energy for

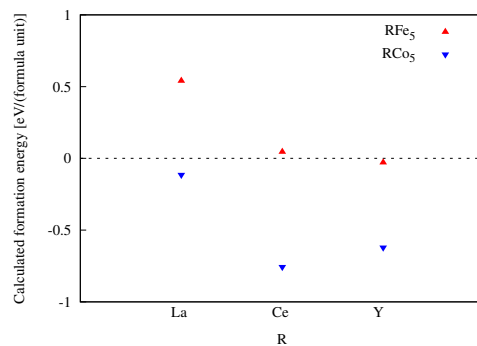


FIG. 1. Calculated formation energy for  $\text{RT}_5$  (R=Ce, La, Y and T=Fe and Co).

	calculated results		experimental data	
	$(a, c)$ [ $\text{\AA}$ ]	$V_{\text{cell}}$ [ $\text{\AA}^3$ ]	$(a, c)$ [ $\text{\AA}$ ]	$V_{\text{cell}}$ [ $\text{\AA}^3$ ]
CeCo <sub>5</sub>	(4.89, 4.02)	84.0	(4.93, 4.02)	84.5
LaCo <sub>5</sub>	(5.06, 3.96)	87.7	(5.09, 3.94)	88.3
YCo <sub>5</sub>	(4.92, 3.95)	83.2	(4.93, 3.99)	84.0
CeFe <sub>5</sub>	(5.06, 4.10)	91.1		N/A
LaFe <sub>5</sub>	(5.19, 4.08)	95.0		N/A
YFe <sub>5</sub>	(5.08, 3.99)	88.8		N/A

TABLE I. Optimized lattice constants and unit-cell volume  $V_{\text{cell}}$  for  $\text{RT}_5$  (R=Ce, La, Y and T=Co, Fe). The experimental data are taken and rounded up to the 3rd digit as quoted in Ref. 21.

$\text{RFe}_5$  running into the positive region. The relative trend between  $\text{LaCo}_5$  and  $\text{YCo}_5$ ,

$$|\Delta E[\text{LaCo}_5]| < |\Delta E[\text{YCo}_5]|$$

shows that the smaller rare-earth elements in the overall trend of lanthanide contraction comes with the better structure stability. Most notable difference between  $\text{LaCo}_5$  and  $\text{YCo}_5$  lies in the radius of rare-earth element, with La being the largest rare earth element and Y being as small as typical heavy rare earth elements like Dy in the trend of lanthanide contraction. It is reasonable for La-based compounds having the enlarged lattice with La sitting on the peak in the size of rare-earth atoms to become relatively fragile against the anticipated magnetovolume effect when combined with the strong  $3d$ -electron magnetization coming from Fe-group elements, since there would be relatively less margin for the chemical bonds to hold on against the volume expansion as imposed by magnetization. In this regard, the relatively small size of  $\text{Ce}^{4+}$  actually gives an advantage on Ce-based ferromagnets at least for the structure stability.

	calculated results		expt.
	$M$ [ $\mu_B$ /(f.u.)]	$M$ [Tesla]	$M$ [Tesla]
CeCo <sub>5</sub>	6.03	0.837	0.77
LaCo <sub>5</sub>	7.03	0.934	0.91
YCo <sub>5</sub>	7.22	1.01	1.09
CeFe <sub>5</sub>	10.6	1.36	N/A
LaFe <sub>5</sub>	11.7	1.43	N/A
YFe <sub>5</sub>	10.7	1.41	N/A

TABLE II. Calculated magnetization for  $RT_5$  ( $R=Ce, La, Y,$  and  $T=Co, Fe$ ). Experimental data for magnetization in Tesla is taken from Ref. 22.

## B. Magnetization

Calculated magnetization as a result of the structure optimization is summarized in Table II. Total magnetic moments per formula unit which occupies the unit cell is normalized by the volume of the unit cell to yield the magnetization measured in Tesla which is of direct relevance for REPM's. The quantitative agreement between the results from *ab initio* structure optimization and experiments for the magnetization in Tesla is seen up to two digits. The realistic energy scales for the cohesion and magnetism seem to be properly taken into account in the present description.

Nature of ferromagnetism can be inspected from calculated total density of states (DOS) as shown in Fig. 2. Only for the fictitious  $YFe_5$ , weak ferromagnetism with a non-negligible amount of majority-spin states on the Fermi level is seen. All of the other compounds show strong ferromagnetism with the  $d$ -electron majority-spin states all below the Fermi level which means that ferromagnetic order is basically saturated there and there is little space for further enhancing magnetization e.g. by mixing Fe and Co to follow the celebrated Slater-Pauling curve. We note that our DOS for  $CeCo_5$  look at variance with what is shown in one of the previous works<sup>21</sup> where their DOS could point to the possible weak ferromagnetism in  $CeCo_5$ . We have actually verified in our calculations that Slater-Pauling curve is not observed for  $Ce(Co,Fe)_5$ <sup>23</sup> so indeed weak ferromagnetism does not seem to be the case at least for the optimized  $CeCo_5$  in our calculations. Since the electronic states near the Fermi level can sensitively depend on the details of calculation setup it could be reasonable to get some variant results for  $CeCo_5$  that may reside almost on a border line between weak ferromagnetism and strong ferromagnetism.

## C. Magnetic anisotropy energy (MAE)

On top of the optimized crystal structure, magnetic anisotropy energy is inspected from first principles by monitoring the energy as a function of the angle between

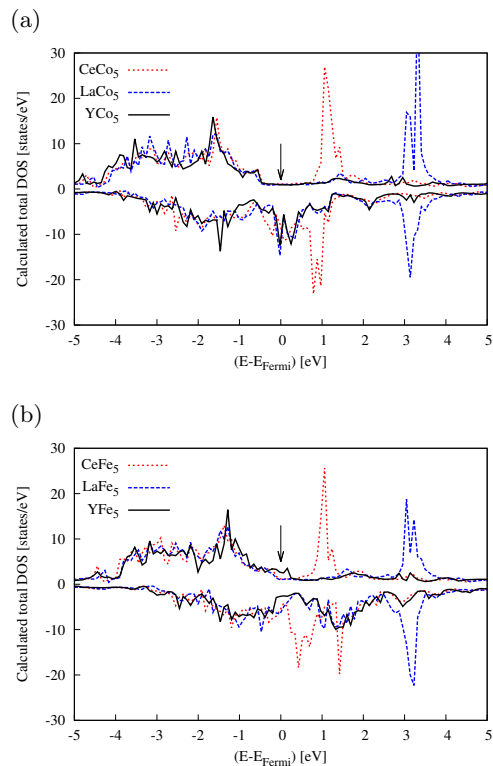


FIG. 2. (Color online) Calculated total density of states for (a)  $RCo_5$  and (b)  $RFe_5$  ( $R=Ce, La,$  and  $Y$ ). The arrow in the figure points to the majority-spin states on the Fermi level.

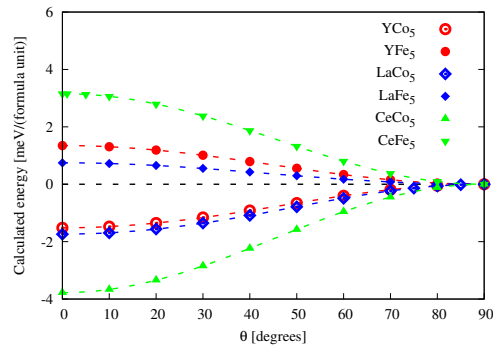


FIG. 3. (Color online) angle dependence of the calculated energy with the zero point being set at the bottom of the calculated total energy. Here the angle is made between the bulk magnetization direction and the crystallographic  $c$ -axis. Overall  $RCo_5$  show uni-axial magnetic anisotropy while  $RFe_5$ 's have easy-direction along the  $ab$ -plane. Dotted lines are fits of Eq. (1) in the text to the calculated data points. The results of such fits are summarized in Table III.

constrained magnetization and the crystallographic  $c$ -axis under the presence of spin-orbit interaction. The results are shown in Fig. 3. Uni-axial magnetic anisotropy of  $RCo_5$  is switched into easy-plane magnetic anisotropy with  $RFe_5$ . Calculated energy as a function of the magnetization direction as shown in Fig. 3 is fitted to the

	$K$ [meV/(formula unit)]	$p$	$q$
CeCo <sub>5</sub>	3.79(2)	-0.0181(2)	0.004(4)
LaCo <sub>5</sub>	1.737(1)	-0.162(4)	$q \equiv 0$
YCo <sub>5</sub>	1.5171(6)	-0.077(2)	$q \equiv 0$
CeFe <sub>5</sub>	-4.39(6)	-0.0130(3)	0.28(1)
LaFe <sub>5</sub>	-0.7471(7)	0.073(4)	$q \equiv 0$
YFe <sub>5</sub>	-1.34706(3)	-0.00103(8)	$q \equiv 0$

TABLE III. Calculated magnetic anisotropy energy and the coefficient of the higher order terms for RT<sub>5</sub> (R=Ce, La, Y and T= Co, Fe).

following relation

$$E_{\text{aniso}} = -K [(1 - p - q) \cos^2 \theta + p \cos^4 \theta + q \cos^6 \theta] \quad (1)$$

to extract the magnetic anisotropy energy together with the higher-order terms. The fit results are summarized in Table III. The absolute values of  $K$  show a significant underestimate as compared to experiments, which seems to be reasonable for *ab initio* calculations for  $3d$ -electron magnetic anisotropy. Without special treatment such as orbital polarization, LDA/GGA+U, or self-interaction correction, it is not easy to quantitatively match the calculated MAE to the experimentally observed range<sup>24</sup>.

For the moment we focus on qualitative trends in the extracted parameters. It is to be noted for the  $4f$ -electron part that relatively strong anisotropy is found for Ce-based compounds as compared to La or Y-based compounds even though the  $4f$ -electrons are presumably in a delocalized state. In Fig. 2 the majority-spin state for Ce, seen on the opposite side to the majority-spin of Co or Fe, has a significant contribution above and below the Fermi level which means  $4f$ -electrons are half-localized as are  $3d$ -electrons in Fe and Co. Thus they contribute positively to the bulk anisotropy.

Turning to the  $3d$ -electron part, it is seen that all Fe-based compounds end up with easy-plane anisotropy: this is not quite interesting in the context of REPM. Given that Fe-rich compounds come with poor structure stability and loss of uni-axial magnetic anisotropy, relatively strong magnetization does not help by itself and an optimal chemical composition for REPM would rather lie on the Co-rich side. Quantitatively identifying the location of an optimal point on a continuum of chemical composition axis is addressed in a separate work<sup>23</sup>.

Remarkably, the coefficient of the extracted higher-order coefficient in YCo<sub>5</sub> is in agreement with the past experimental claim stating  $K_2/K_1 = -0.021$ <sup>25</sup> where  $K_1 \equiv K(1 - p)$  and  $K_2 \equiv Kp$  in our notation. Our data amounts to  $K_2/K_1 = -0.071$  and the sign of the higher order contribution has been correctly reproduced.

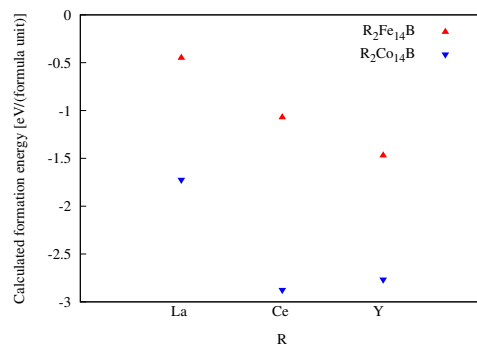


FIG. 4. Calculated formation energy for R<sub>2</sub>T<sub>14</sub>B (R=Ce, La, Y and T=Fe,Co). The data for (La,Ce)<sub>2</sub>Fe<sub>14</sub>B and Y<sub>2</sub>(Fe,Co)<sub>14</sub>B are taken from Ref. 19 and Ref. 18, respectively.

## IV. DISCUSSIONS

Comparison between what we have seen for RT<sub>5</sub> and analogous data for the champion magnet compound family, R<sub>2</sub>T<sub>14</sub>B, is described in Sec. IV A which reveals the trends with respect to the crystal structure variety where the latter was reached in quest for a way to enlarge the interatomic spacing between Fe<sup>26</sup>. Implications on the materials design for REPM's are discussed in Sec. IV B taking the recently discussed materials family RT<sub>12</sub><sup>27</sup> as the possible playground for the application of the proposed principles.

### A. Comparison with R<sub>2</sub>T<sub>14</sub>B

#### 1. Formation energy

Calculated formation energy for Ce<sub>2</sub>Co<sub>14</sub>B and La<sub>2</sub>Co<sub>14</sub>B are shown in Fig. 4 together with the data for R<sub>2</sub>Fe<sub>14</sub>B (R=Ce and La)<sup>19</sup> and Y<sub>2</sub>T<sub>14</sub>B (T=Co, Fe)<sup>18</sup> for the convenience of getting an overview. Parallel trends with what is seen in Fig. 1 is obvious, with the most significant difference being the overall offset to push down everything down to the negative region of the formation energy. Even with the intrinsic trend that Fe-based compounds come with the relatively poor structure stability, with the particular crystal structure of R<sub>2</sub>T<sub>14</sub>B they can be stabilized except for La<sub>2</sub>Fe<sub>14</sub>B that looks perhaps too close to being on the verge to the positive side of the formation energy.

Absence of Ce<sub>2</sub>Co<sub>14</sub>B in the experimental literature is a mystery as long as we look at the trends of the formation energy. The absolute value of the calculated formation energy for Ce<sub>2</sub>Co<sub>14</sub>B is more than double of that for Ce<sub>2</sub>Fe<sub>14</sub>B, which is consistent with one of the recent claims<sup>28</sup>. Presumably, other compounds may compete against Ce<sub>2</sub>Co<sub>14</sub>B in getting bulk-stabilized, or something beyond the present level of electronic structure cal-

	calculated results			expt.
	$M$ [ $\mu_B$ /(f.u.)]	$V_{\text{cell}}$ [ $\text{\AA}^3$ ]	$(a, c)$ $\text{\AA}$	$(a, c)$ $\text{\AA}$
Ce <sub>2</sub> Co <sub>14</sub> B	16.64	865	(8.596, 11.73)	N/A
La <sub>2</sub> Co <sub>14</sub> B	18.67	891	(8.635, 11.96)	(8.67, 12.01)
Y <sub>2</sub> Co <sub>14</sub> B	18.70	855	(8.560, 11.68)	(8.60, 11.71)
Ce <sub>2</sub> Fe <sub>14</sub> B	29.95	936	(8.797, 12.11)	(8.76, 12.11)
La <sub>2</sub> Fe <sub>14</sub> B	31.92	961	(8.835, 12.33)	(8.82, 12.34)
Y <sub>2</sub> Fe <sub>14</sub> B	31.47	922	(8.775, 11.99)	(8.76, 12.00)

TABLE IV. Optimized lattice constants and unit-cell volume for  $R_2T_{14}B$  ( $R=\text{Ce, La, Y}$  and  $T=\text{Co, Fe}$ ). The data for  $(\text{La,Ce})_2\text{Fe}_{14}\text{B}$  and  $\text{Y}_2(\text{Fe,Co})_{14}\text{B}$  are partly taken from Ref. 19 and Ref. 18, respectively. Experimental lattice constants are taken from Ref. 1.

calculations might be at work in real experiments: in the present calculations we have plainly put  $4f$ -electrons of Ce into the valence state which is not always justified.

## 2. Magnetization

Calculated magnetization for  $R_2T_{14}B$  are summarized in Table IV and V together with the optimized lattice information for the convenience of calculating magnetization in Tesla. Again the data for  $R_2\text{Fe}_{14}\text{B}$  ( $R=\text{Ce}$  and  $\text{La}$ ) and  $\text{Y}_2T_{14}\text{B}$  ( $T=\text{Co, Fe}$ ) are taken from Refs. 19 and 18, respectively. It is seen that the optimized lattice constants are in quantitative agreement with the experimental ones up to three digits while calculated magnetization in Tesla sometimes has an overestimate where the deviation from experimental data amounts to a few tens of %. Practically it has not been easy to let the calculations for  $R_2\text{Co}_{14}\text{B}$  converge. It actually took having an initial magnetic state with each Co atom starting with unrealistically large magnetic polarization to reach any sensibly converged results in our *ab initio* structure optimization for  $R_2\text{Co}_{14}\text{B}$  so far. In this way it might have been reasonable to have ended up with an overestimate of magnetization and also this may indicate that our description of  $3d$ -electron state may not have been as precise as has been achieved for Fe-based counterparts<sup>19</sup>. Anyways relative trends e.g. between  $\text{La}_2\text{Co}_{14}\text{B}$  and  $\text{Y}_2\text{Co}_{14}\text{B}$  seems to have been satisfactorily described.

## 3. Magnetic anisotropy energy

Magnetic anisotropy energy for  $\text{Ce}_2\text{Co}_{14}\text{B}$  and  $\text{La}_2\text{Co}_{14}\text{B}$  can be inspected in an analogous way to what was done for  $\text{RT}_5$  in Sec. III C. The results are shown in Fig. 5 together with the counterpart data for  $\text{Ce}_2\text{Fe}_{14}\text{B}$  and  $\text{La}_2\text{Fe}_{14}\text{B}$  as partly taken from Ref. 19. It actually took lifting off the constraints on magnetic moments on Ce and La for the fully relativistic runs of  $R_2\text{Co}_{14}\text{B}$  ( $R=\text{Ce}$  and  $\text{La}$ ) to reach convergence. The same was true

	calc.	expt.
Ce <sub>2</sub> Co <sub>14</sub> B	0.896	N/A
La <sub>2</sub> Co <sub>14</sub> B	0.977	0.741
Y <sub>2</sub> Co <sub>14</sub> B	1.02	0.848
Ce <sub>2</sub> Fe <sub>14</sub> B	1.49	1.47
La <sub>2</sub> Fe <sub>14</sub> B	1.55	1.48
Y <sub>2</sub> Fe <sub>14</sub> B	1.59	1.59

TABLE V. Calculated magnetization in Tesla for  $R_2T_{14}B$  ( $R=\text{Ce, La, Y}$  and  $T=\text{Co, Fe}$ ). Experimental data for  $M$  at  $T = 4.2$  K is taken from Ref. 1 for  $R_2\text{Fe}_{14}\text{B}$  and Ref. 29 for  $R_2\text{Co}_{14}\text{B}$ .

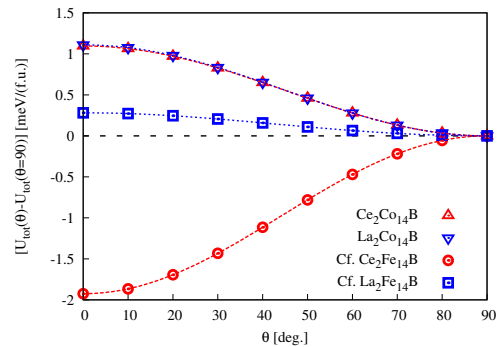


FIG. 5. Angle-dependence of calculated energy of  $R_2\text{Co}_{14}\text{B}$  ( $R=\text{Ce}$  and  $\text{La}$ ). For a comparison, analogous data for  $R_2\text{Fe}_{14}\text{B}$  are included partly from Ref. 19.

for  $\text{La}_2\text{Fe}_{14}\text{B}$  in Ref. 19 but it was not actually the case for  $\text{Ce}_2\text{Fe}_{14}\text{B}$  in Ref. 19 - here, just for a comparison on an equal footing, results from fully relativistic calculations for  $\text{Ce}_2\text{Fe}_{14}\text{B}$  without the constraints on magnetic moments on Ce are presented. The difference from the fully relativistic calculations for  $\text{Ce}_2\text{Fe}_{14}\text{B}$  in Ref. 19 where the constraints on the direction of magnetic moments were all imposed on Ce and Fe is seen only quantitatively in the absolute value of  $K$  with a slightly smaller number coming up here. The other parameters show qualitatively similar behavior, with positive  $p$  and negative  $q$  coming up in the same range in the absolute value  $|p| \simeq |q|$  for  $\text{Ce}_2\text{Fe}_{14}\text{B}$ , irrespectively of the constraints on the magnetic moments on Ce being applied (Ref. 19) or not (here).

It is remarkable that we hardly observe any differ-

	$K$ [meV/(formula unit)]	$p$	$q$
Ce <sub>2</sub> Co <sub>14</sub> B	-1.21(1)	-0.0188(4)	0.089(9)
La <sub>2</sub> Co <sub>14</sub> B	-1.10974(5)	-0.0072(2)	$q \equiv 0$
Ce <sub>2</sub> Fe <sub>14</sub> B	1.83(1)	0.0360(6)	-0.051(7)
La <sub>2</sub> Fe <sub>14</sub> B	-0.28106(7)	0.098(1)	$q \equiv 0$

TABLE VI. Calculated magnetic anisotropy energy and the coefficient of the higher order terms for  $R_2T_{14}B$ .

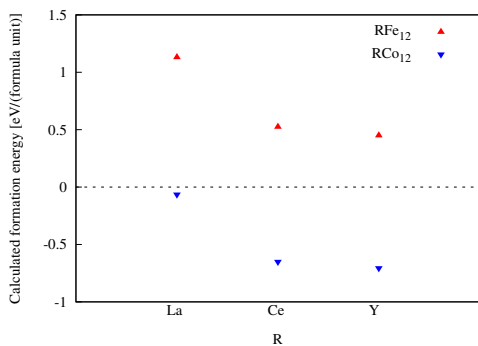


FIG. 6. Calculated formation energy for  $RT_{12}$  ( $R=\text{Ce, La, Y}$  and  $T=\text{Co, Fe}$ ).

calculated results				
	$M$ [ $\mu_B$ /(f.u.)]	$(a, c)$ $\text{\AA}$	$V_{\text{cell}}$	$M$ [Tesla]
CeCo <sub>12</sub>	17.99	(8.33, 4.65)	161	1.30
LaCo <sub>12</sub>	18.95	(8.40, 4.67)	165	1.34
YCo <sub>12</sub>	19.05	(8.28, 4.66)	160	1.39
CeFe <sub>12</sub>	27.15	(8.58, 4.73)	174	1.82
LaFe <sub>12</sub>	27.7	(8.66, 4.73)	177	1.82
YFe <sub>12</sub>	27.2	(8.51, 4.73)	171	1.85

TABLE VII. Calculated magnetization and optimized lattice constants and unit-cell volume for  $RT_{12}$  ( $R=\text{Ce, La, Y}$  and  $T=\text{Co, Fe}$ ).

ence between  $\text{Ce}_2\text{Co}_{14}\text{B}$  and  $\text{La}_2\text{Co}_{14}\text{B}$  concerning their easy-plane bulk MAE in the absolute value, except for the qualitative behavior of higher-order terms. This is in strong contrast to the difference between  $\text{Ce}_2\text{Fe}_{14}\text{B}$  and  $\text{La}_2\text{Fe}_{14}\text{B}$  where even the sign of bulk anisotropy is flipped between them.

### B. Implications on the possible new REPM based on $RT_{12}$

In the past five years there has been a surge in the interests in  $RT_{12}$  compounds<sup>27</sup> that can potentially go beyond the champion magnet compounds  $\text{R}_2\text{T}_{14}\text{B}$  in the intrinsic properties. Here the structure stability has been traded off to demonstrate the real-material implementation of case studies to go beyond  $\text{Nd}_2\text{Fe}_{14}\text{B}$ <sup>30–32</sup>. Recent interests focus on the quest for gaining both of satisfactorily good magnetic properties and sufficient structure stability to move on to a working REPM in industrial applications. Here we take a brief look at the outcome of *ab initio* structure optimization for  $RT_{12}$  with  $R=\text{Ce, La, Y}$  and  $T=\text{Co, Fe}$  and see to what extent we might be

able to recycle what we have seen with  $\text{RT}_5$  and  $\text{R}_2\text{T}_{14}\text{B}$ .

Calculated formation energy for  $RT_{12}$  is shown in Fig. 6. The overall trend in the structure stability is qualitatively shared among  $\text{RT}_5$  and  $\text{R}_2\text{T}_{14}\text{B}$  in the sense that a) Co-based compounds are generally more stable than Fe-based compounds and b) smaller rare-earth elements give more stable structure. Combined with calculated magnetization in Tesla as summarized in Table VII points to  $\text{CeCo}_{12}$  and  $\text{YCo}_{12}$  that can provide a good compromise coming with both reasonably good magnetization and comfortably as stable as  $\text{CeCo}_5$  as long as the calculated formation energy shows. Apparently  $\text{RT}_{12}$  resembles  $\text{RT}_5$  in several respects rather than being considered as an alternative to  $\text{R}_2\text{T}_{14}\text{B}$ . It might be feasible to pursue the possible line toward a mid-class REPM on the basis of  $\text{CeCo}_{12}$  possibly with a small addition of Fe for gaining magnetization not to the extent where the structure stability is ruined, in an analogous way to the development of Fe-doped  $\text{YCo}_5$ <sup>17,23,33</sup>.

## V. CONCLUSIONS AND OUTLOOK

Intrinsic trade-off between structure stability and magnetization has been inspected from first principles for  $\text{RT}_5$ . Comparison has been done with the champion magnet compounds  $\text{R}_2\text{T}_{14}\text{B}$  and the recently focused materials family  $RT_{12}$ . Detailed characterization of the fictitious compound  $\text{Ce}_2\text{Co}_{14}\text{B}$  has been done for the first time to the best of the author’s knowledge. Throughout the calculations covering materials family, roles of Ce in helping structure stabilization and positive contribution to the intrinsic magnetic anisotropy has been elucidated on the basis of calculated electronic structure and we identify  $\text{CeCo}_{12}$  as a possible starting point for the fabrication of a next-generation mid-range REPM.

## ACKNOWLEDGMENTS

MM’s work in ISSP, Univ. of Tokyo is supported by Toyota Motor Corporation. Helpful interactions with A. Marmodoro, A. Ernst, C. E. Patrick, J. B. Staunton, M. Hoffmann, H. Akai, T. Miyake, Y. Harashima in related projects and useful comments given by T. Ozaki, F. Ishii for *ab initio* calculations employing OpenMX are gratefully acknowledged. Part of the present work was supported by JSPS KAKENHI Grant No. 15K13525 and the Elements Strategy Initiative Center for Magnetic Materials (ESICMM) under the outsourcing project of the Ministry of Education, Culture, Sports, Science and Technology (MEXT), Japan. Numerical calculations were done on ISSP supercomputer center, Univ. of Tokyo.

<sup>1</sup> J. F. Herbst, Rev. Mod. Phys. **63**, 819 (1991).

<sup>2</sup> H. S. Li and J. M. D. Coey, Handbook of Magnetic Materials, **6**, Ed. K. H. J. Buschow, Ch. 1.

- <sup>3</sup> <http://www.openmx-square.org/>
- <sup>4</sup> T. Ozaki, Phys. Rev. B. **67**, 155108, (2003).
- <sup>5</sup> T. Ozaki and H. Kino, Phys. Rev. B **69**, 195113 (2004).
- <sup>6</sup> T. Ozaki and H. Kino, Phys. Rev. B **72**, 045121 (2005).
- <sup>7</sup> T. V. T. Duy and T. Ozaki, Comput. Phys. Commun. **185**, 777 (2014).
- <sup>8</sup> K. Lejaeghere, G. Bihlmayer, T. Björkman, P. Blaha, S. Blügel, V. Blum, D. Caliste, I.E. Castelli, S.J. Clark, A. Dal Corso, S. de Gironcoli, T. Deutsch, J.K. Dewhurst, I. Di Marco, C. Draxl, M. Dulak, O. Eriksson, J.A. Flores-Livas, K.F. Garrity, L. Genovese, P. Giannozzi, M. Giantomassi, S. Goedecker, X. Gonze, O. Grånäs, E.K. Gross, A. Gulans, F. Gygi, D.R. Hamann, P.J. Hasnip, N.A. Holzwarth, D. Işsan, D.B. Jochym, F. Jollet, D. Jones, G. Kresse, K. Koepf, E. Küçükbenli, Y.O. Kvashnin, I.L. Loch, S. Lubeck, M. Marsman, N. Marzari, U. Nitzsche, L. Nordström, T. Ozaki, L. Paulatto, C.J. Pickard, W. Poelmans, M.I. Probert, K. Refson, M. Richter, G.M. Rignanese, S. Saha, M. Scheffler, M. Schlipf, K. Schwarz, S. Sharma, F. Tavazza, P. Thunström, A. Tkatchenko, M. Torrent, D. Vanderbilt, M.J. van Setten, V. Van Speybroeck, J.M. Wills, J.R. Yates, G.X. Zhang, and S. Cottenier, Science **351**, aad3000 (2016).
- <sup>9</sup> I. Morrison, D.M. Bylander, L. Kleinman, Phys. Rev. B **47**, 6728 (1993).
- <sup>10</sup> G. Theurich and N.A. Hill, Phys. Rev. B **64**, 073106 (2001).
- <sup>11</sup> J. P. Perdew, K. Burke, and M. Ernzerhof, Phys. Rev. Lett. **77**, 3865 (1996).
- <sup>12</sup> H. Shishido *et al.*, in preparation.
- <sup>13</sup> J. Schweizer and F. Tasset, J. Phys. F: Met. Phys. **10**, 2799 (1980).
- <sup>14</sup> M. Matsumoto, R. Banerjee, J. B. Staunton, Phys. Rev. B **90**, 054421 (2014).
- <sup>15</sup> M. Matsumoto, R. Banerjee, J. B. Staunton, JPS Conf. Proc. **5**, 011004 (2015).
- <sup>16</sup> M. Matsumoto and H. Akai, preprint [arXiv:1812.04842].
- <sup>17</sup> C. E. Patrick, M. Matsumoto, J. B. Staunton, J. Magn. Magn. Mater. **477**, 147 (2019).
- <sup>18</sup> M. Matsumoto, preprint [arXiv:1812.10945].
- <sup>19</sup> M. Matsumoto, M. Ito, N. Sakuma, M. Yano, T. Shoji, H. Akai, preprint [arXiv:1901.10119].
- <sup>20</sup> Z. D. Zhang, W. Liu, J. P. Liu, and D. J. Sellmyer, J. Phys. D: Appl. Phys. **33**, R217 (2000).
- <sup>21</sup> L. Nordström, O. Eriksson, M. S. S. Brooks, and B. Johansson, Phys. Rev. B **41**, 9111 (1990).
- <sup>22</sup> K. Ohashi, J. Japan Inst. Metals **76**, 96 (2012) (in Japanese except for abstract, key words, and figure captions).
- <sup>23</sup> MM, M. Hoffmann, *et al.*, in preparation.
- <sup>24</sup> P. Larson and I. I. Mazin, J. Appl. Phys. **93**, 6888 (2003).
- <sup>25</sup> J. M. Alameda, D. Givord, R. Lemaire, Q. Lu: J. Appl. Phys. **52** (1981) 2079.
- <sup>26</sup> M. Sagawa, S. Fujimura, N. Togawa, H. Yamamoto, and Y. Matsuura, J. Appl. Phys. **55**, 2083 (1984); M. Sagawa, private communications (2017).
- <sup>27</sup> For a review, see Y. Hirayama, T. Miyake, and K. Hono, JOM **67**, 1344 (2015).
- <sup>28</sup> J. F. Herbst and L. G. Hector Jr., J. Alloys Compd. **693**, 238 (2017).
- <sup>29</sup> K. H. J. Buschow, Ferromagnetic Materials **4**, Eds. E. P. Wohlfarth and K. H. J. Buschow, Ch. 1 (1988).
- <sup>30</sup> T. Miyake, K. Terakura, Y. Harashima, H. Kino, and S. Ishibashi, J. Phys. Soc. Jpn. **83**, 043702 (2014).
- <sup>31</sup> Y. Hirayama, Y. K. Takahashi, S. Hirose, and K. Hono, Scr. Mater. **95**, 70 (2015).
- <sup>32</sup> Y. Hirayama, Y. K. Takahashi, S. Hirose, and K. Hono, Scr. Mater. **138**, 62 (2017).
- <sup>33</sup> P. Tozman, M. Venkatesan, G. A. Zickler, J. Fidler, J. M. D. Coey, Appl. Phys. Lett. **107** 032405 (2015); P. Tozman, M. Venkatesan, J. M. D. Coey, AIP Adv. **6**, 056016 (2016); M. Soderžnik, M. Korent, K. Žagar Soderžnik J.-M. Dubois, P. Tozman, M. Venkatesan, J. M. D. Coey, S. Kobe, J. Magn. Magn. Mater. **460**, 401 (2018).